Electronic Supplementary Information

From metal-organic framework to carbon: toward controlled hierarchical pore structures via a double-templates approach

Jian-Ke Sun and Qiang Xu*

National Institute of Advanced Industrial Science and Technology (AIST), Ikeda, Osaka 563-8577, Japan

****

Experimental Section

Chemicals and Instrumentation. All chemicals were from commercial and used without further purification. 2-aminoterephthalic acid (Tokyo Chemical Industry Co., Ltd.), aluminum chloride hexahydrate ($AlCl_3 \cdot 6H_2O$, Tokyo Chemical Industry Co., Ltd.), copper(II) nitrate trihydrate ($Cu(NO_3)_2 \cdot 3H_2O$, Kishida Chemical Co., Ltd.), N, N-dimethylaformamide (DMF, Tokyo Chemical Industry Co., Ltd.), aqueous hydrofluoric acid (HF, 46%, Kishida Chemical Co., Ltd), hydrochloric acid (HCl, 37%, Wako Pure Chemical Industries, Ltd.), anhydrous n-hexane (Sigma-Aldrich) and ethanol (C_2H_5OH, 99%) were used as received. Powder X-ray diffraction (PXRD) measurements were carried out on a Mac Science MXP3 V diffractometer with Ni filtered Cu-Kα radiation (λ = 0.15406 nm) (40 kV, 20 mA). Scanning electron microscopic (SEM) analyses were carried with a Hitachi S-5000 field emission scanning electron microscope. Transmission electron microscope (TEM, FEI TECNAI G2) and energy-dispersive X-ray spectroscopy (EDS) were applied for the detailed microstructure and composition information. X-ray photoelectron spectroscopic (XPS) analyses were carried out on a Shimadzu ESCA-3400 X-ray photoelectron spectrometer using an Mg K α source (10 kV, 10 mA). The surface area measurements were performed with N_2 adsorption/desorption isotherms at liquid nitrogen temperature (77 K) after dehydration under vacuum at 150 ºC for 12 h using automatic volumetric adsorption equipment (Belsorp-max). The pore volume was calculated by a single point method at $P/P_0 = 0.99$. The H_2 and CO_2 adsorption/desorption isotherms were measured at 77 and 273 K, respectively, using automatic volumetric adsorption equipment (Belsorp-mini II).

Synthesis of Al-MIL-101-NH_2. The synthesis of Al-MIL-101-NH_2 is according to the previous method[1] with a modified procedure. A typical synthesis of Al-MIL-101-NH_2 was performed as follows: in a 100 mL round bottom flask 272 mg (1.5 mmol) of 2-aminoterephthalic acid was dissolved in 60 mL of DMF and heated to 110 °C in an oil bath. 724 mg (3 mmol) of $AlCl_3 \cdot 6H_2O$ was added in 7 equal portions with a time delay of 15 min between each two additions. After the last portion was added, the temperature was kept at 110 °C for 3 h under stirring and for an additional 16 h without stirring. After cooling down to room temperature, the yellow solid was isolated by filtration, washed with 100 mL of DMF and ethanol for three times, and then further purified by treatment in ethanol at 80 ºC for 16 h and washed with hot ethanol. The resultant yellow solid was finally dried for 10 h at 200 °C under vacuum for further use.

Synthesis of XCu@Al-MIL-101-NH_2 (X = 0.5, 1, 2). Encapsulation of Cu^{2+} templates was carried out using the double-solvents method.[2] Typically, 300 mg of dehydrated Al-MIL-101-NH_2 was suspended in 40 mL of dry n-hexane as hydrophobic solvent and the mixture was sonicated for about 30 min until it became homogeneous. After stirring for 1 h, 0.3 mL of aqueous $Cu(NO)_3 \cdot 3H_2O$ solution with desired concentrations (19, 38 and 76 mg/mL for 0.5Cu@Al-MIL-101-NH_2, 1Cu@Al-MIL-101-NH_2 and 2Cu@Al-MIL-101-NH_2, respectively.) as the hydrophilic solvent was added dropwise over a period of 50 min with constant vigorous stirring. The resulting solution was continuously stirred for 3 h. After stirring, the solid which settled down to the bottom of the sample vial was isolated from the supernatant by decanting and drying in air at room temperature. The as-synthesized sample was further dried at 120 °C under vacuum for 12 h.

Preparation of Carbon Sample MIL-C. The dehydrated Al-MIL-101-NH_2 sample (300 mg) was immersed in dry n-hexane and sonicated for about 30 min until it became homogeneous. Then the sample was isolated and dried in vacuum at 120 °C for 12 h. The dried sample was transferred into a ceramic boat and placed into a

temperature-programmed furnace under an argon flow, heated from room temperature to 800 °C in 80 min, and then kept at 800 °C for 5 h and cooled down to room temperature. The resultant black material was washed several times with a HF (23 wt%) solution, followed by washing with plenty of distilled water and dried at 80 °C for 12 h to afford MIL-C.

Preparation of Carbon Sample MIL-C-X. Typically, the dried XCu@Al-MIL-101-NH_2 (X = 0.5, 1, 2) sample (300 mg) was transferred into a ceramic boat and placed into a temperature-programmed furnace under an argon flow, heated from room temperature to 800 °C in 80 min, and then kept at 800 °C for 5 h and cooled down to room temperature. The resultant black material was washed several times with a HCl (37 wt%) solution, followed by washing with a HF (23 wt%) solution. Then the sample was washed with plenty of distilled and dried at 80 °C for 12 h to afford MIL-C-X (X=0.5, 1, 2).

Capacitor Construction. All electrochemical measurements were carried out in a two-electrode cell (capacitor) with an aqueous solution of sulfuric acid (1.0 M) as electrolyte (each electrode containing 2.0 mg carbon without adding any binder and conductive agents), in which a glassy paper separator was sandwiched between two electrodes and platinum plates were used as electric collectors. Two identical electrodes were adopted as cathode and anode for the cell configuration.

Electrochemical Measurements. The electrochemical experiments were performed under ambient conditions. Before the measurements, the capacitor cell was evacuated for 3 h to allow the active material fully soaked in the electrolyte. Cyclic voltammograms at different sweep rates for the capacitor were carried out on a Solartron electrochemical workstation (SI1287). The specific capacitance is calculated according to the following equation (1):

$$C = 2 \times \Delta Q / (\Delta V \times m) \qquad (1)$$

where ΔQ is the charge integrated from the whole voltage range, ΔV is the whole voltage difference, and m is the mass of carbon on an electrode. Galvanostatic charge/discharge examinations at various current densities were performed on a Solartron electrochemical workstation (SI1287) and a voltage range of -0.5 to 0.5 V was set. Specific capacitance of each electrode was calculated according to the following equation (2):

$$C = 2 \times I \times \Delta t / (\Delta V \times m) \qquad (2)$$

where I is the discharge current, Δt is the discharge time from 0.5 to -0.5 V, ΔV is the voltage difference within the discharge time Δt, and m is the mass of carbon on an electrode. The factor of two in these equations comes from the fact that the total capacitance measured from the test cells is the sum of two equivalent single electrode capacitors in series.

Additional Figures and Data

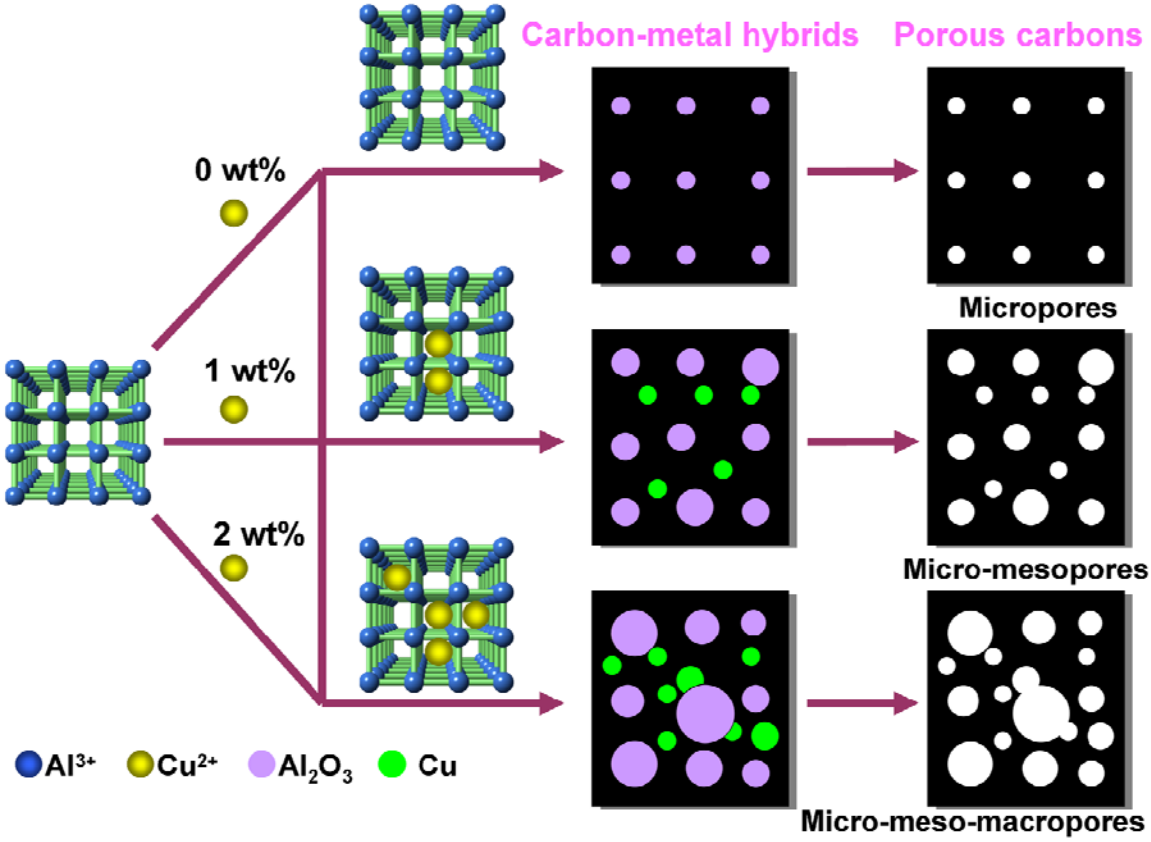

Scheme S1. Schematical illustration of fine-tuning of the pore structures of MOF-derived carbons on the basis of a double-templates approach. The preloaded metal ions (Cu^{2+}) in MOF not only play a role of pore-forming agent by *in situ* transforming into the Cu nanoparticles during the carbonization process, but also trigger the size and phase transformation of metal oxides (Al_2O_3) generated from MOFs in the resultant carbon-metal hybrids due to a doping effect. The sizes of Al_2O_3 particles depend on the amounts of preloaded Cu^{2+} ions prior to carbonization. The controllable particle sizes will produce porous carbons with desired hierarchical pore structures after removal of the metal species from carbon matrix.

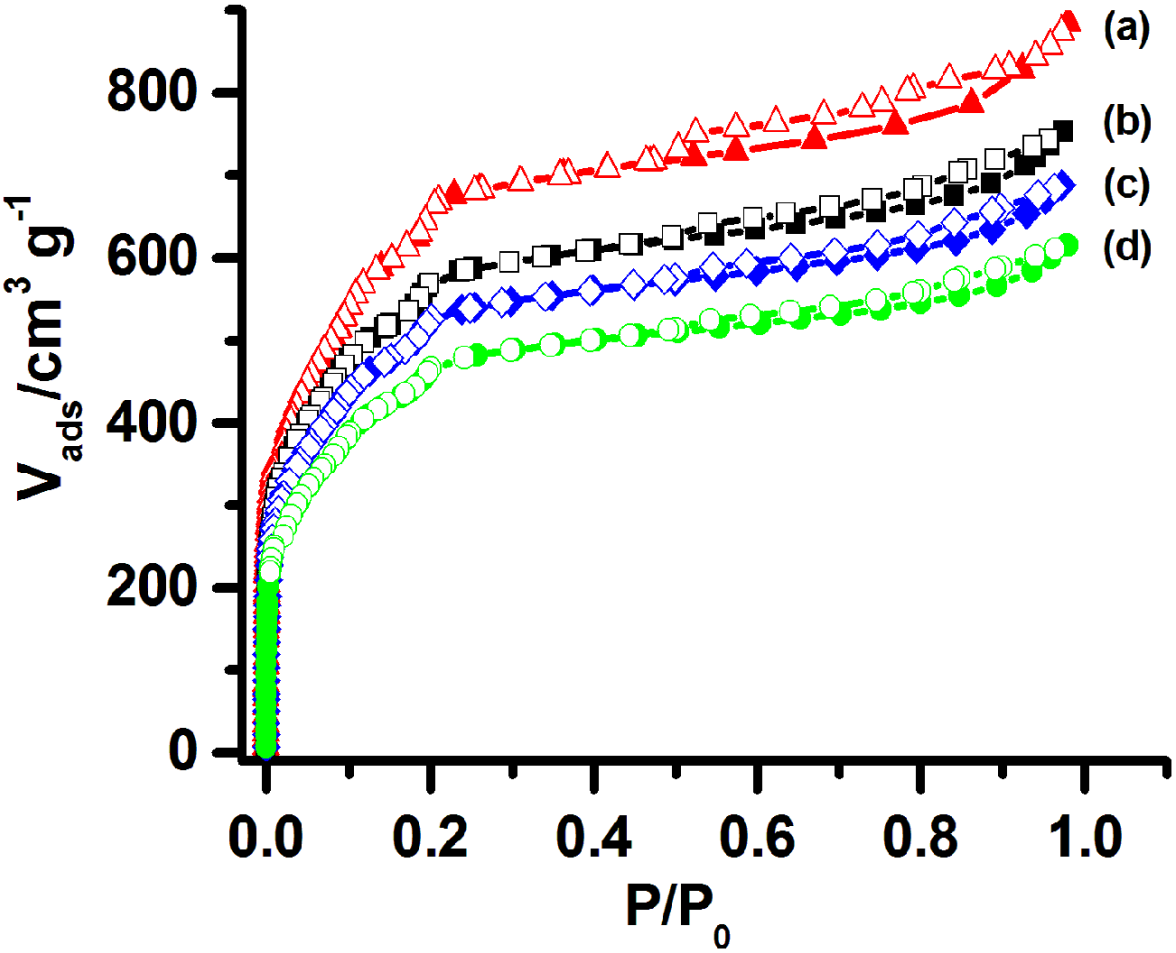

Figure S1. N_2 sorption isotherms of (a) as-synthesized MIL-101-Al-NH_2, (b) 0.5Cu@MIL-101-Al-NH_2, (c) 1Cu@MIL-101-Al-NH_2, and (d) 2Cu@MIL-101-Al-NH_2 at 77 K. Filled and open symbols represent adsorption and desorption branches, respectively.

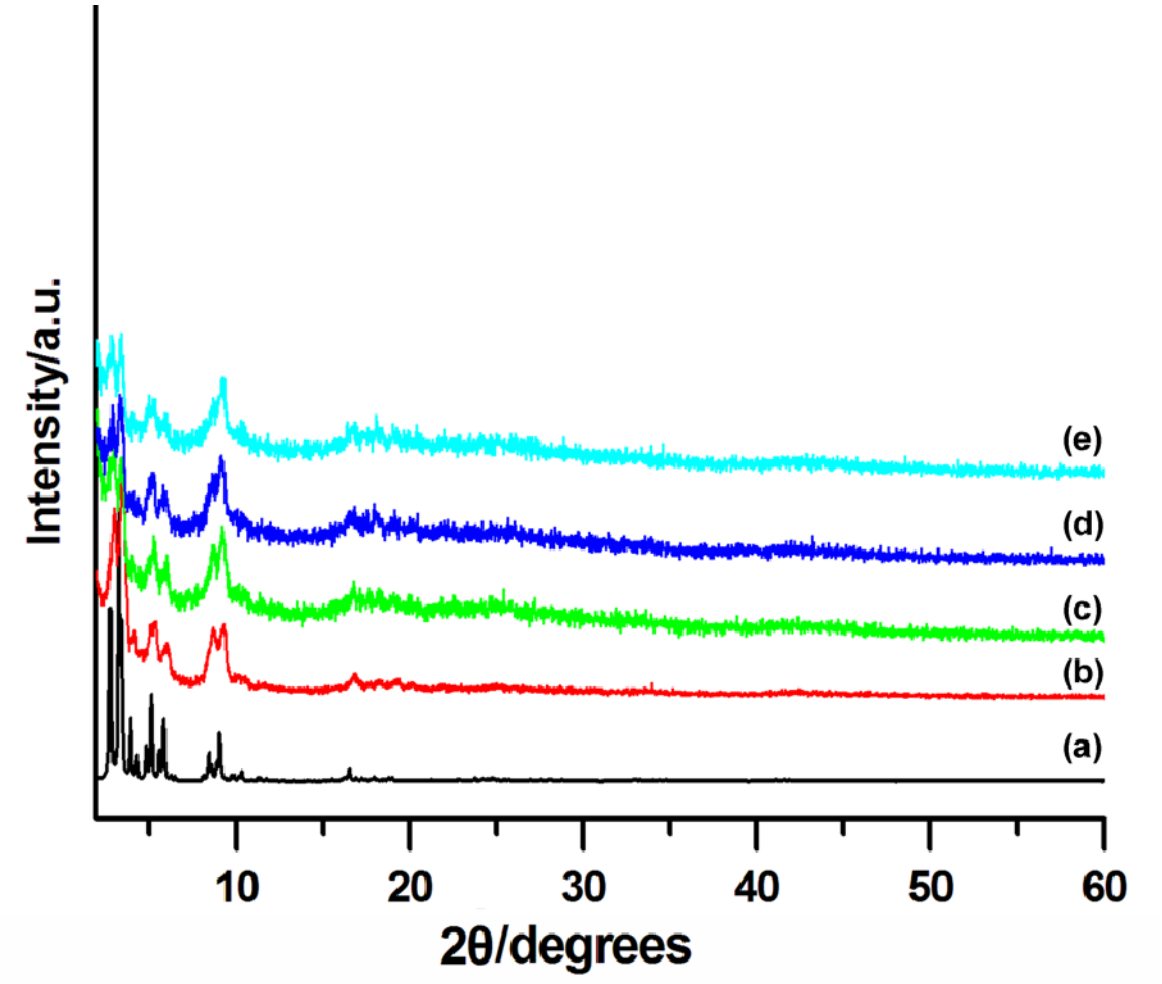

Figure S2. PXRD patterns of (a) simulated MIL-101-Al-NH_2, (b) as-synthesized MIL-101-Al-NH_2, (c) 0.5Cu@MIL-101-Al-NH_2, (d) 1Cu@ MIL-101-Al-NH_2 and (e) 2Cu@MIL-101-Al-NH_2.

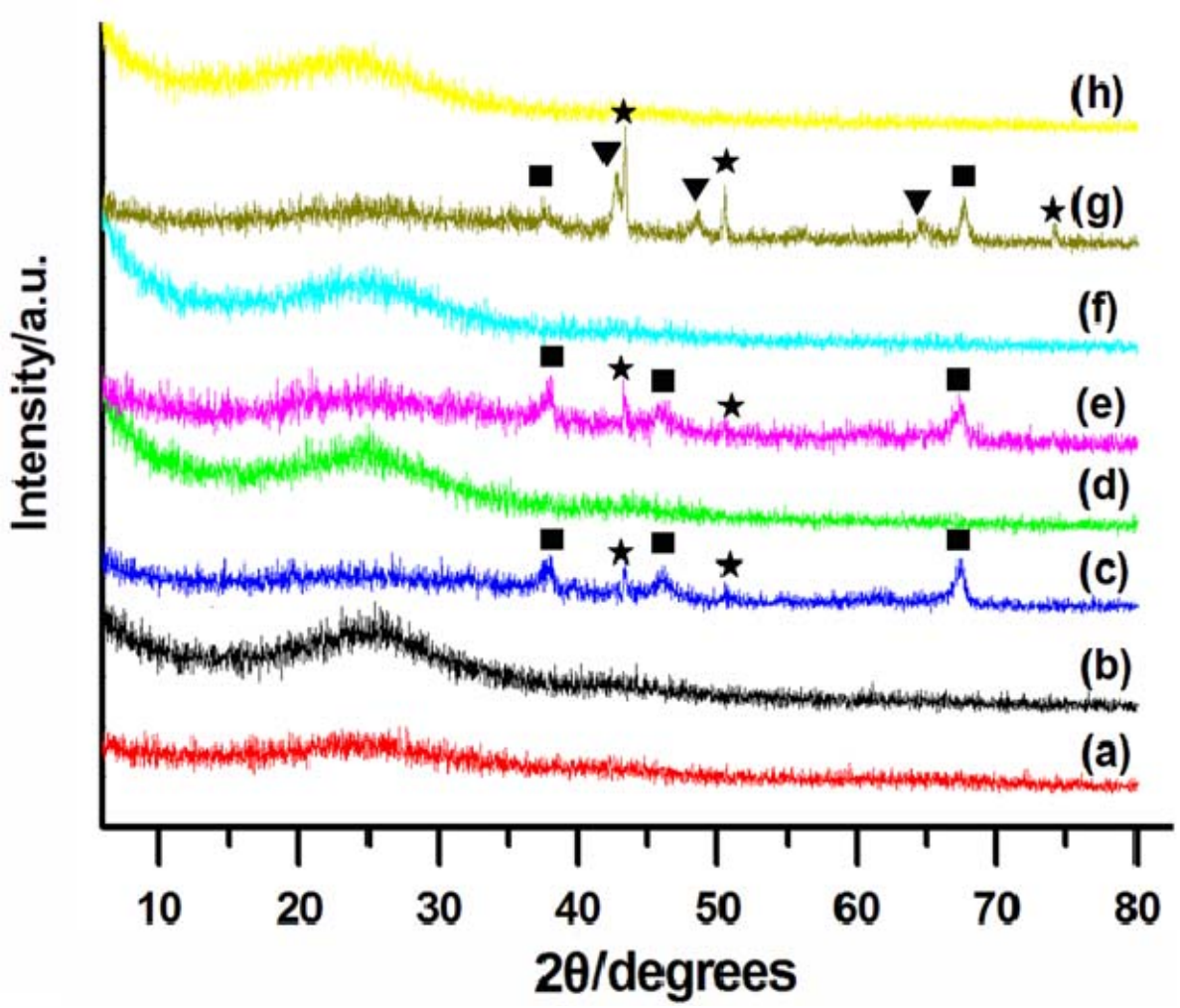

Figure S3. PXRD patterns for the raw carbons derived from MOFs and the purified carbons after washing with the acids. (a) Raw carbon derived from Al-MIL-101-NH_2, (b) MIL-C, (c) raw carbon derived from 0.5Cu@Al-MIL-101-NH_2, (d) MIL-C-0.5, (e) raw carbon derived from 1Cu@Al-MIL-101-NH_2, (f) MIL-C-1, (g) raw carbon derived from 2Cu@Al-MIL-101-NH_2, (h) MIL-C-2. The Al_2O_3 (PDF#10-0425) (■), (PDF#26-0031) (▼), Cu (PDF#04-0836) (★) are highlighted with different symbols.

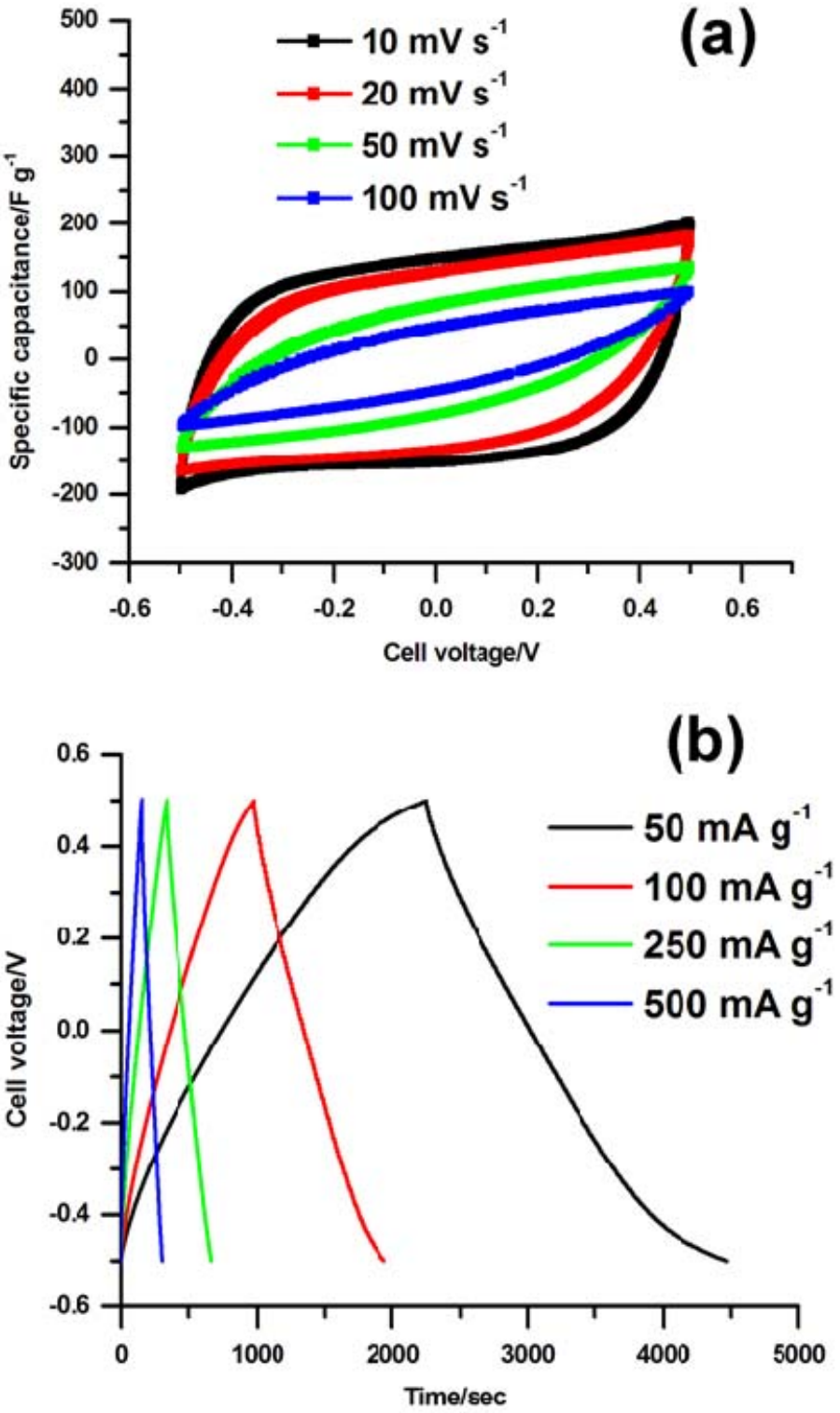

Figure S4. (a) Cyclic voltammograms at different scan rates and (b) galvanostatic charge/discharge curves at different current densities for MIL-C.

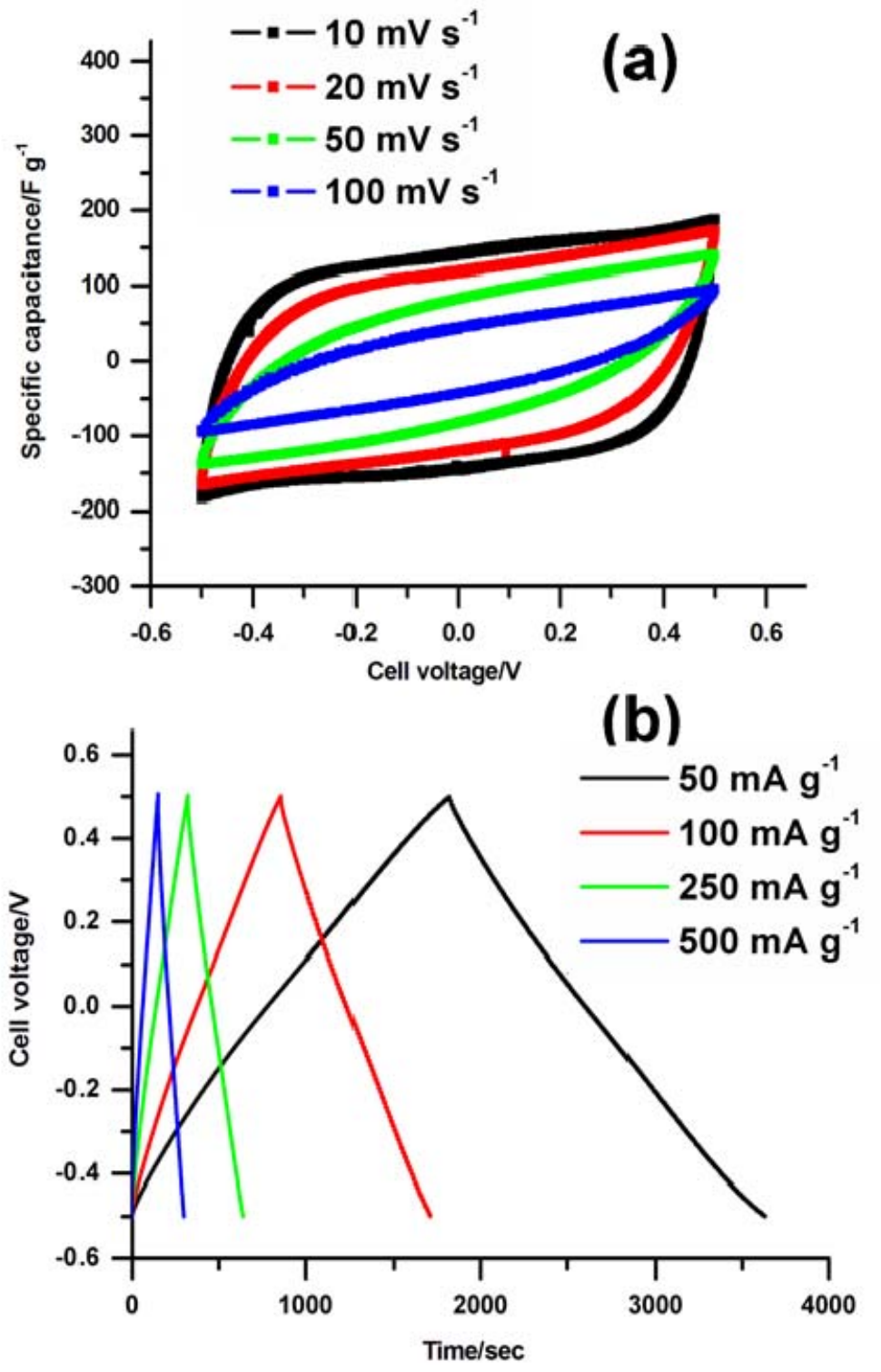

Figure S5. (a) Cyclic voltammograms at different scan rates and (b) galvanostatic charge/discharge curves at different current densities for MIL-C-0.5.

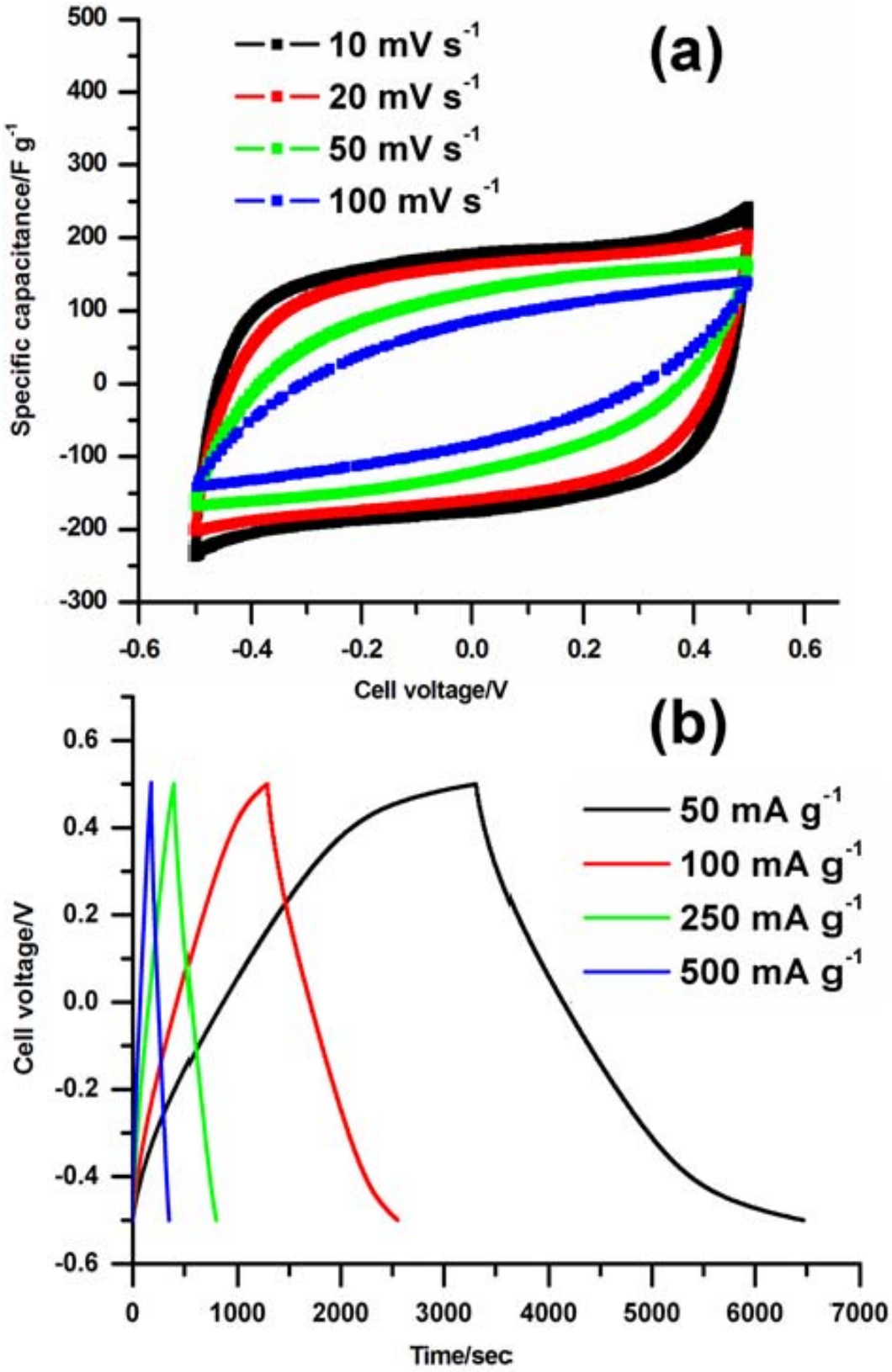

Figure S6. (a) Cyclic voltammograms at different scan rates and (b) galvanostatic charge/discharge curves at different current densities for MIL-C-1.

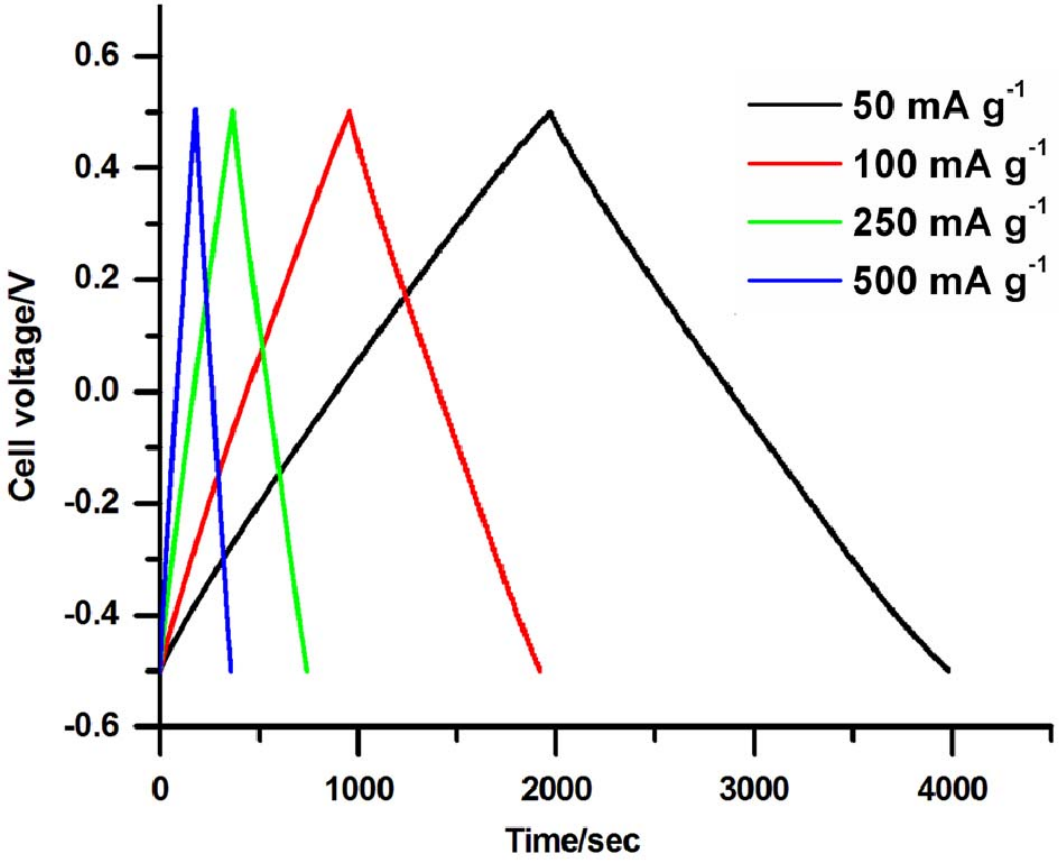

Figure S7. Galvanostatic charge-discharge profiles at different current densities for MIL-C-2.

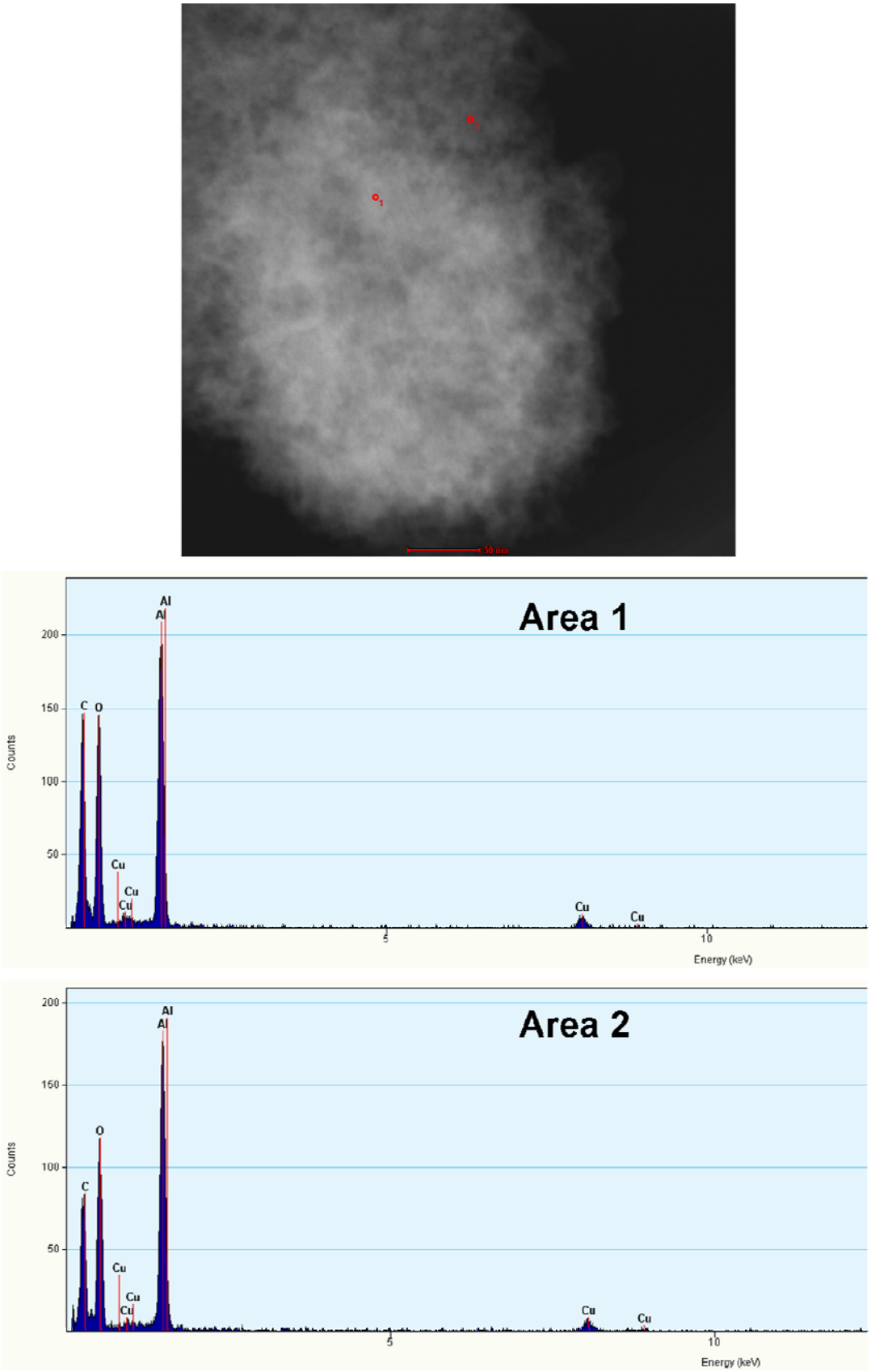

Figure S8. HAADF–STEM image of the raw carbon derived from MIL-101-Al-NH_2, and the corresponding EDS spectra for the selected areas in the raw carbon. The Cu peaks arise from the TEM grid (Cu).

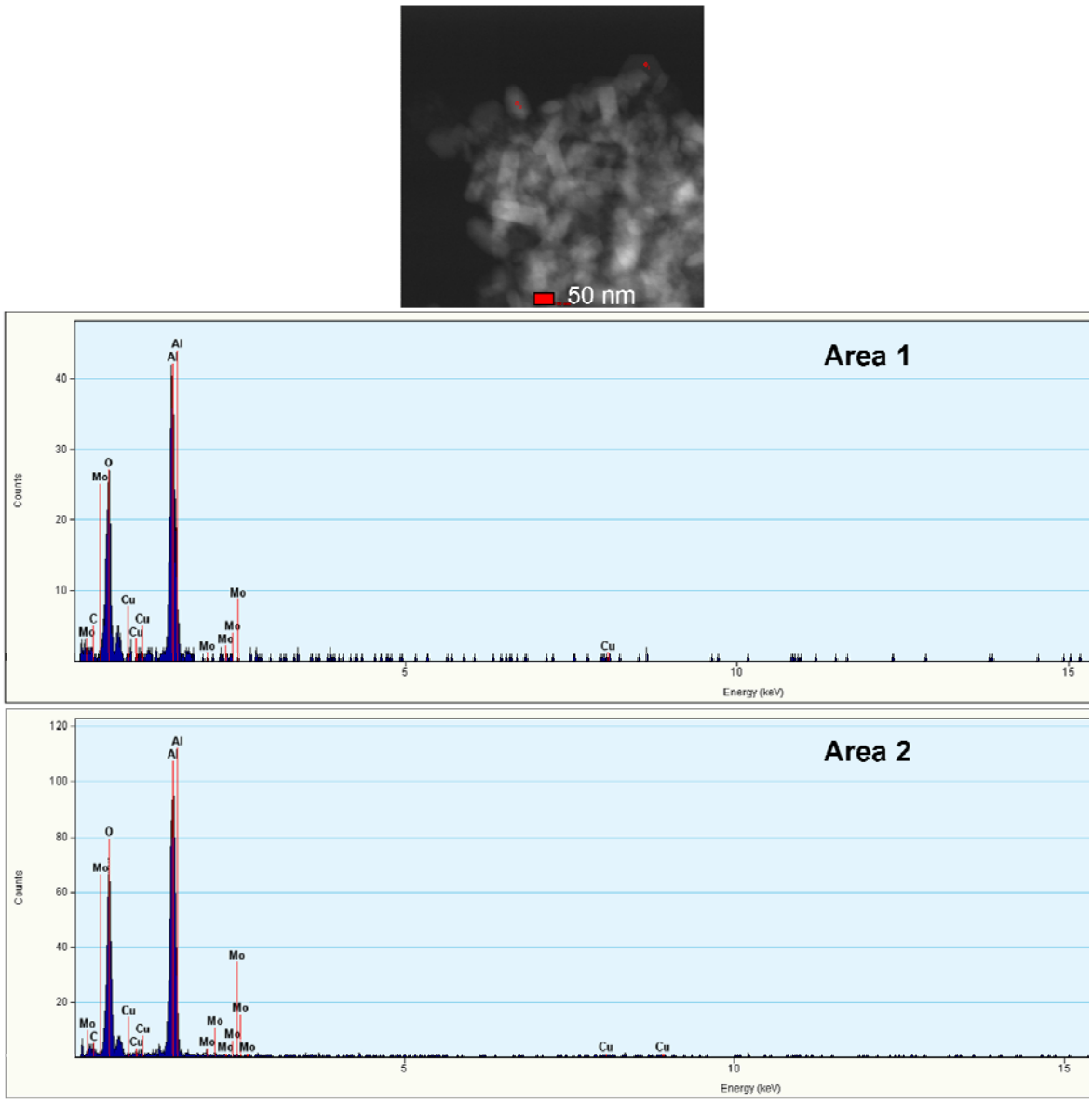

Figure S9. HAADF–STEM image of the raw carbon derived from 2Cu@MIL-101-Al-NH_2, and the corresponding EDS spectra for the selected areas in the raw carbon. The Mo peaks arise from the TEM grid (Mo). The Cu signal can be detected on the selected sites of large crystals, indicating that a small amount of Cu^{2+} may be incorporated into the Al_2O_3 domain at an initial nucleation stage.

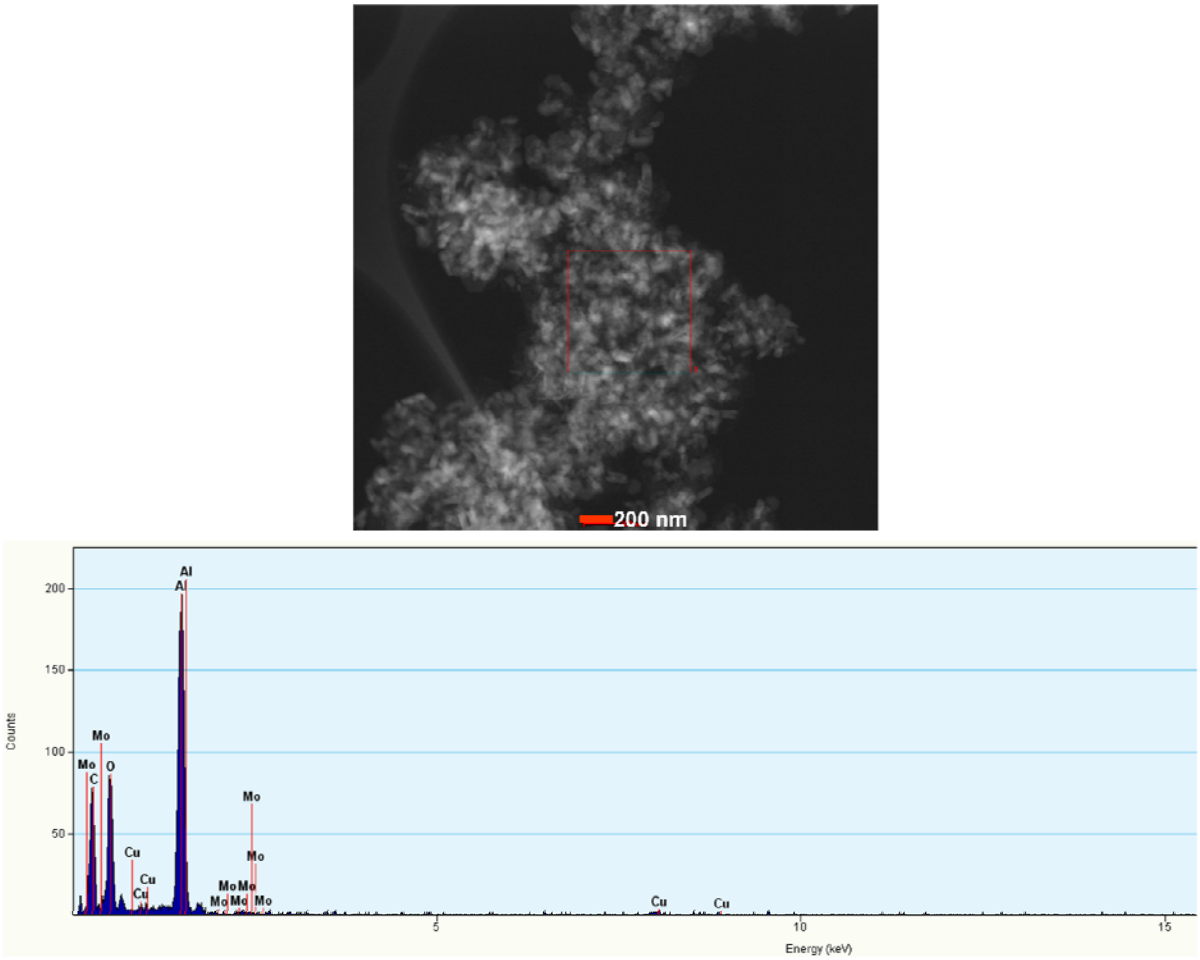

Figure S10. Low-magnitude HAADF–STEM image of the raw carbon derived from 2Cu@MIL-101-Al-NH_2, and the corresponding EDS spectrum for the selected area in the raw carbon. The Mo peaks arise from the TEM grid (Mo).

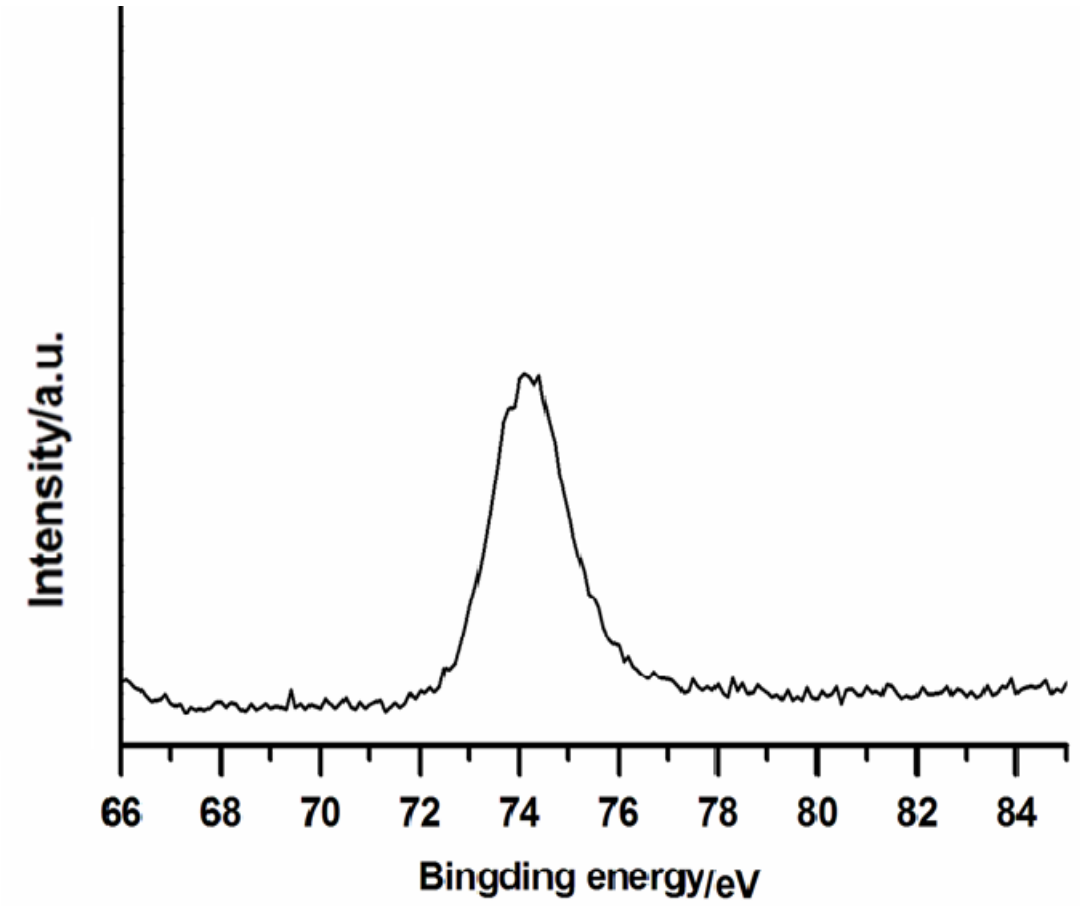

Figure S11. XPS spectrum for Al^{3+} signal in MIL-101-Al-NH_2 derived raw carbon.

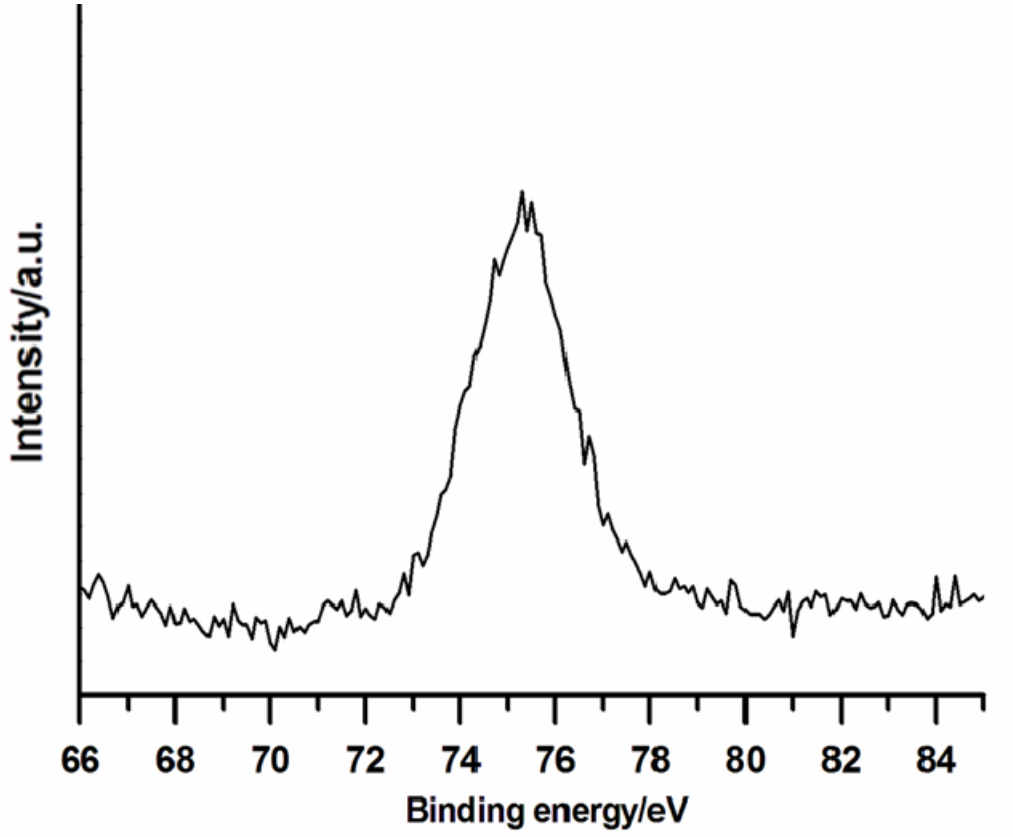

Figure S12. XPS spectrum for Al^{3+} signal in 2Cu@MIL-101-Al-NH_2 derived raw carbon.

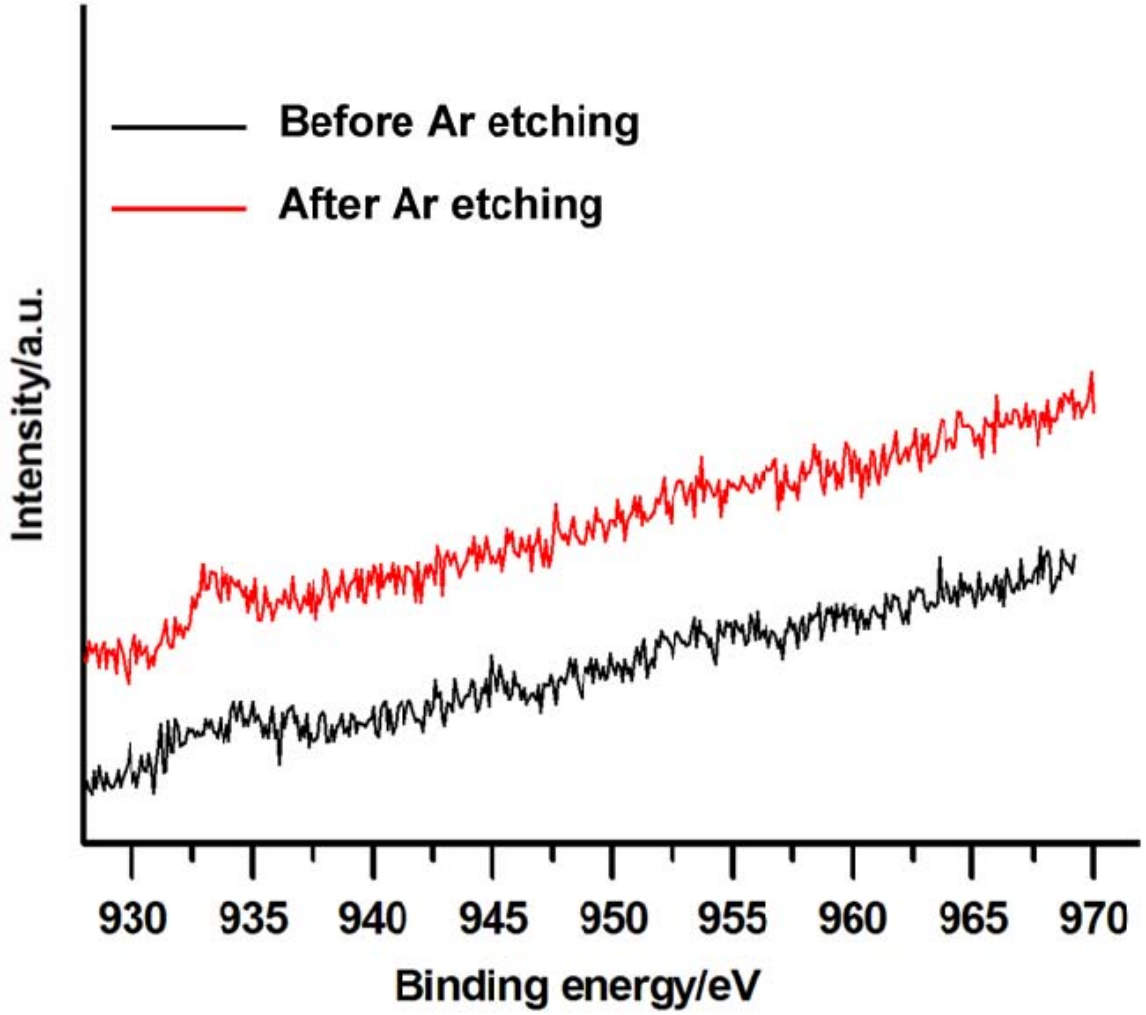

Figure S13. XPS Spectra for Cu signals in 2Cu@MIL-101-Al-NH_2 derived raw carbon before and after Ar etching (240 min). The peak at 933.3 eV with a satellite peak at 945.1 eV for Cu $2p_{3/2}$ are observed,[3] which is attributed to a thin oxidized cover formed during the exposure of the raw carbon to air. Well-defined peaks at 932.8 eV corresponding to metallic Cu can be detected after Ar etching for 240 min and no satellite peak is observed, suggesting zero-valent state of copper in the raw carbon.[4]

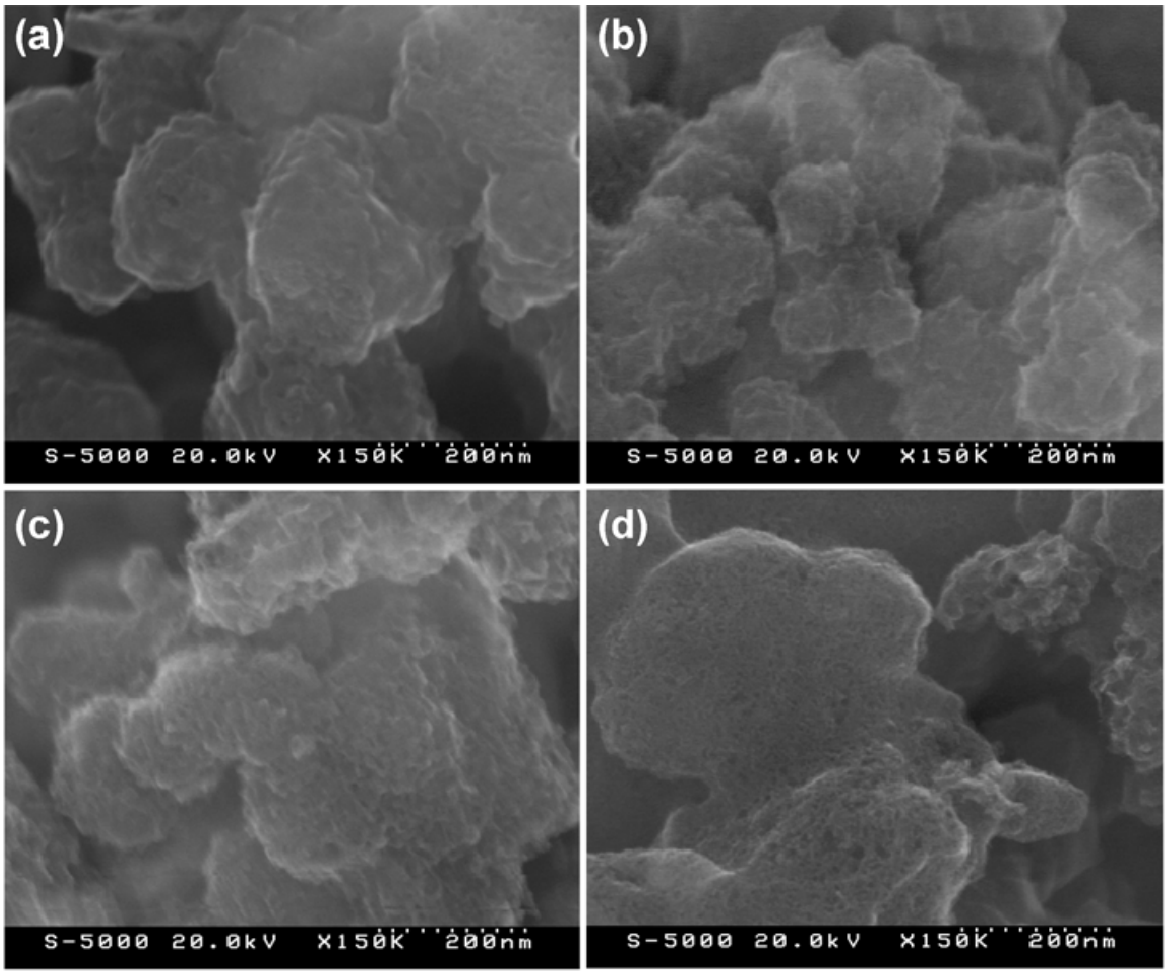

Figure S14. SEM images of (a) MIL-C, (b) MIL-C-0.5, (c) MIL-C-1, (d) MIL-C-2.

Table S1. Summary of the surface areas and pore volume distributions for the carbons

Sample	Specific surface area[a] (m^2 g^{-1})	Total pore volume[b] (cm^3 g^{-1})	Meso-Macropore volume[c] (cm^3 g^{-1})	Micropore volume[d] (cm^3 g^{-1})
MIL-C	1328	0.7981	0.2177	0.5804
MIL-C-0.5	1699	1.2066	0.6497	0.5569
MIL-C-1	2116	1.6237	1.0687	0.5550
MIL-C-2	1397	2.3961	1.9276	0.4685

[a] Calculated from the BET surface area analysis.
[b] Calculated by a single point method at $P/P_0 = 0.99$.
[c] Calculated using a t-plot method.
[d] Calculated by subtracting the total pore volume with the meso-/macropore volumes.

Table S2. Specific capacitances at different sweep rates in various carbon-based supercapacitors with 1.0 M H_2SO_4 solution as electrolyte

Sweep rate (mV s^{-1})	Specific capacitance (F g^{-1})			
	MIL-C	MIL-C-0.5	MIL-C-1	MIL-C-2
10	145	143	180	185
20	127	120	162	178
50	81	84	123	172
100	46	43	83	171

References:

1 M. Hartmann and M. Fischer, *Microporous Mesoporous Mater.,* 2012, **164**, 38.
2 A. Aijaz, A. Karkamkar, Y. J. Choi, N. Tsumori, E. Rönnebro, T. Autrey, H. Shioyama and Q. Xu, *J. Am. Chem. Soc.,* 2012, **134**, 13926.
3 L. Hu, H.Y. Hong, M. Li, Q. Y. Bao, J. X. Tang, J. F. Ge, J. M. Lu, X. Q. Cao and H. W. Gu, *Chem. Commun.,* 2010, **46**, 8591.
4 S. Jeong, S. H. Lee, Y. J. Jo, S. S. Lee, Y. H. Seo, B. W. Ahn, G. Kim, G. E. Jang, J. U. Park, B. H. Ryu and Y. Choi, *J. Mater. Chem. C,* 2013, **1**, 2704.